DOI: 10.1002/ejic.200700646

1D and 2D Fe^{II} Azide Coordination Polymers with Ferromagnetic Canting

Morsy A. M. Abu-Youssef,*[a] Vratislav Langer,[b] Dominique Luneau,[c,d] Eman Shams,[a] Mohamed A. S. Goher,[a] and Lars Öhrström*[b]

Keywords: Crystal engineering / Bridging ligands / Azides / Magnetic properties / Network compounds / Topology

The two compounds $[Fe^{II}(pyridine)_2(N_3)_2(H_2O)]$ (**1**) and $[Fe^{II}(4\text{-acetylpyridine})_2(N_3)_2]$ (**2**) were prepared. The X-ray crystal structures show end-to-end (EE) bridging azides in both cases with a 1D Fe–NNN–Fe chain for **1** and a 2D Fe–NNN–Fe net in **2**. Both compounds show similar magnetic behaviour where the high-temperature data are consistent with antiferromagnetic couplings and the low-temperature data indicate ferrimagnetic ordering based on spin canting at 20 and 45 K. Compound **2** also shows a hysteresis loop. These findings are compared to the related 3D coordination polymer $[Fe(N_3)_2(4,4'\text{-bipyridine})]$. According to network analyses the latter compound was shown to contain the new uninodal six-connected-network topology $(5^{10}\cdot6^4\cdot7)$-**jsm**.

Introduction

Magnetic materials based on molecular components continue to be attractive and difficult goals for organic and inorganic chemists despite more than 20 years of research on this subject.[1] In recent years there has been much focus on "single-molecule magnets",[2] but lately a new room temperature (high T_c) magnetic material has also been reported.[3] Coordination chemistry underpins most of the successes in the area, although the structural features of some of the most interesting compounds are not fully known,[4] while some of the compounds with bridging cyanide ligands and high T_c are relatively well understood.[5,6]

Such successes have so far not been obtained with the azide ligand, another suitable bridging anion, which, unlike the cyanide ligand, can show several coordination-bridging modes, the most common of these being the $\mu_{1,3}$ (end-to-end, EE) and the $\mu_{1,1}$ (end-on, EO). However, strong magnetic couplings are common features of M-azido systems and therefore the structure and magnetism of coordination polymers based on transition metals and azide ions continue to attract attention.[7]

From a structural point of view, new 3D nets have been prepared,[8,9] and in terms of magnetism, hysteretic magnetic bistability,[10] a two-dimensional homometallic ferrimagnet[11] and long-range ferromagnetic ordering at approximately 6 K[12] have recently been reported for such compounds.

Fe^{II} compounds are of special interest since they may show bistability (spin transitions),[13] but the magnetism may be less straightforward to interpret. Spin-canted magnetism has been reported for $[FeCl_2(pyrimidine)_2]$[14] and also for $[Fe(N_3)_2(pyrimidine)]$,[15] and the two polymorphs of $[Fe(N_3)_2(4,4'\text{-bipyridine})]$[16] have been characterised as metamagnets and ferromagnets at low temperature.

In this article we report on two new Fe^{II} azides exhibiting spin-canted ferromagnetism, $[Fe^{II}(pyridine)_2(N_3)_2(H_2O)]$ (**1**) and $[Fe^{II}(4\text{-acetylpyridine})_2(N_3)]$ (**2**) (ligands shown in Scheme 1). These form related supramolecular 2D nets and both display spin-canted ferromagnetism similar to that described for analogous Mn^{II}[17] and Co^{II}[18] compounds. Moreover, as we analysed the magnetism and compared it to relevant examples in the literature we came across a new 3D-network topology found in the 3D polymorph of $[Fe(N_3)_2(4,4'\text{-bipyridine})]$,[16] which we will also briefly discuss.

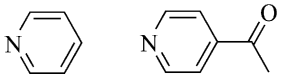

Scheme 1. Ligands used to prepare $[Fe^{II}(pyridine)_2(N_3)_3(H_2O)]$ (**1**) and $[Fe^{II}(4\text{-acetylpyridine})_2(N_3)]$ (**2**).

[a] Chemistry Dept., Faculty of Science, Alexandria University, P. O. Box 426 Ibrahimia, 21321 Alexandria, Egypt
Fax: +20-3-3911794
E-mail: morsy5@link.net
[b] Dept. of Chemical and Biological Engineering, Chalmers Tekniska Högskola, 41296 Göteborg, Sweden
Fax: +46-31-772-3858
E-mail: langer@chalmers.se
ohrstrom@chalmers.se
[c] Université Claude Bernard Lyon 1 – Laboratoire des Multimatériaux et Interfaces (UMR 5615), Campus de La Doua, 69622 Villeurbanne Cedex, France
Fax: +33-472-43-1160
E-mail: luneau@univ-lyon1.fr
[d] CEA–Grenoble – DRFMC – Service de Chimie Inorganique et Biologique, 17 rue des Martyrs, 38054 Grenoble Cedex 9, France

Results and Discussion

Structures

$[Fe^{II}(pyridine)_2(N_3)_2(H_2O)]$ (**1**) crystallises in the orthorhombic space group *Fddd* and crystallographic data are given in Table 1. An ORTEP-type drawing of the molecular unit is shown in Figure 1.

Table 1. Crystallographic data.

Compound	**1**	**2**
Ligand	pyridine	4-acetylpyridine
Formula	$C_{10}H_{12}FeN_8O$	$C_{14}H_{14}FeN_8O_2$
M_r [g mol^{-1}]	316.12	382.18
T [K]	173(2)	173(2)
λ [Å]	0.71073	0.71073
Crystal system	orthorhombic	monoclinic
Space group	*Fddd*	$P2_1/c$
a [Å]	10.8348(1)	11.5723(2)
b [Å]	16.6709(1)	8.3874(2)
c [Å]	30.2343(1)	8.3067(1)
β [°]	90	93.599(1)
V [Å^3]	5461.10(5)	804.67(3)
Z	16	2
ρ_{calcd} [g cm^{-3}]	1.538	1.577
μ [mm^{-1}]	1.114	0.965
F (000)	2592	392
Crystal size [mm]	0.38 × 0.12 × 0.11	0.34 × 0.22 × 0.02
θ [°]	2.34–32.94	3.00–32.82
Measured reflections	22396	13615
Unique reflections	2497	2813
R(int.)	0.0316	0.0363
Completeness [%]	100.0 (θ = 30.00°)	99.6 (θ = 30.00°)
Data/restraints/ parameters	2497/48/112	2813/0/123
GOF on F_2	1.048	1.007
R_1 [$I > 2\sigma(I)$]	0.0294	0.0302
wR_2 [$I > 2\sigma(I)$]	0.0742	0.0739
R_1 (all data)	0.0390	0.0414
wR_2 (all data)	0.0795	0.0798
Largest diff. peak and hole [e Å^{-3}]	0.449, –0.296	0.387, –0.357

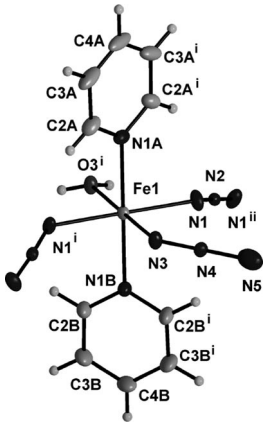

Figure 1. A thermal ellipsoid drawing of $[Fe^{II}(pyridine)_2(N_3)_2(H_2O)]$ (**1**). Ellipsoids are drawn at the 30% probability level. Symmetry codes: (i): $-x + 3/4, -y + 3/4, z$; (ii): $-x + 5/4, y, -z + 1/4$.

The coordination geometry is unremarkable and closely related to that of the Co^{II} compound described in detail in ref.[18] Fe–azide geometric data pertinent to the magnetic properties are: N2–N1–Fe1 133.42(10)°, N1–N2–N1 176.98(18)°, N1–N2 1.1671(11) Å. Tables of geometric data can be obtained from the Cambridge Crystallographic Data Centre (for details see below).

The structure is disordered with alternating water and azide molecules at the twofold axis, and the complexes form 1D-coordination polymer chains along the *a* direction and hydrogen bonded chains along the *b* axis. This results in an alternating coordination/hydrogen bonded (4,4)-2D net, see Figure 2, with iron–iron distances of 5.4763(1) Å and 8.3738(1) Å.

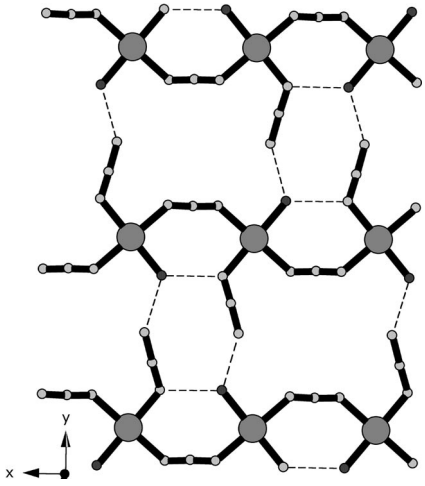

Figure 2. The alternating coordination/hydrogen bonded (4,4)-2D net in $[Fe^{II}(pyridine)_2(N_3)_2(H_2O)]$ (**1**). Hydrogen-bond geometries are: O3–H2···N5 2.6352(12) Å and 166(2)°; O3–H1···N3 2.814(2) Å and 165(3)°. Note that these hydrogen bonded water molecules and azide ligands are disordered over the same sites. Hydrogen atoms and pyridine groups have been omitted for clarity.

The layers are parallel, but translated [0.25,0.25,0] relative to each other, and connected via π–π and σ–π interactions, see Figure 3. Inter-sheet Fe···Fe distances are 8.3890(3) and 9.0465(3) Å, and result in a body-centred-"cubic" packing of the iron ions.

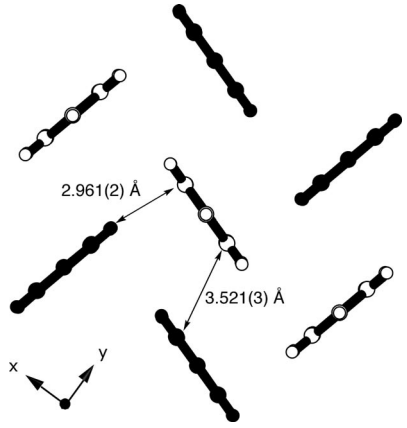

Figure 3. The π–π and σ–π interactions between two nets in **1**. Black and white pyridine groups correspond to different layers.

$[Fe^{II}(4\text{-acetylpyridine})_2(N_3)_2]$ (**2**) crystallises in the monoclinic space group $P2_1/c$ and crystallographic data are given in Table 1. An ORTEP-type drawing of the molecular unit

is shown in Figure 4. The coordination geometry is unremarkable and closely related to that of the Co^{II} compound described in detail in ref.[18] Fe–azide geometric data relevant to the magnetic properties are: N11–N12 1.1695(16) Å, N12–N13 1.1826(15) Å, N12–N11–Fe1 149.69(11)°, N11–N12–N13 176.83(13)°, N12–N13–Fe1 127.24(10)°. Tables of geometric data can be obtained from the Cambridge Crystallographic Data Centre (for details see below).

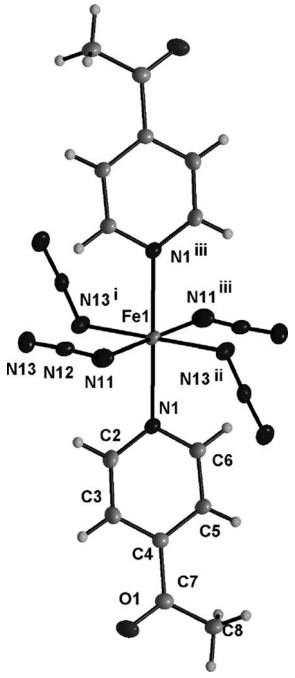

Figure 4. A thermal ellipsoid drawing of $[Fe^{II}(4\text{-acetylpyridine})_2(N_3)_2]$ (**2**). Ellipsoids are drawn at the 50% probability level. Symmetry code: (i): $x, -y + 3/2, z - 1/2$.

In contrast to **1**, compound **2** forms a 2D-coordination polymer consisting of corrugated-square grids where all the Fe^{II} ions are connected by the same type of end-to-end azide bridges, see Figure 5. These sheets are similar to those in **1**, giving iron–iron distances of 5.9023(1) Å.

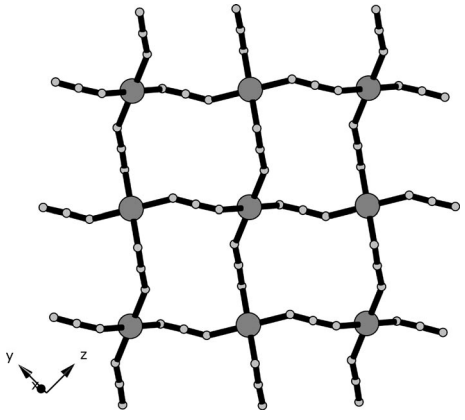

Figure 5. The 2D-square grid $[Fe^{II}(4\text{-acetylpyridine})_2(N_3)_2]$ (**2**). Hydrogen atoms and pyridine groups have been omitted for clarity.

However, the introduction of the acetyl group completely changes the sheet-to-sheet packing, instead of π–π and σ–π interactions we now have weak hydrogen bonds [C3–H3···O1: 3.510(2) Å and 151°; C8–H8A···O1: 3.472(2) Å and 156°] connecting the layers, see Figure 6 (although some π–π stacking is also present). As a consequence, the aromatic groups are now tilted 23° to the 2D network to probably ensure a better packing (**2** is in fact more dense than **1**). These hydrogen-bond "tapes" running between the sheets are furthermore supported by a strong dipole–dipole interaction between the carbonyl groups [O1···C7 3.222(2) Å, O1–C5···O1–C5 dihedral 0.0° by symmetry].

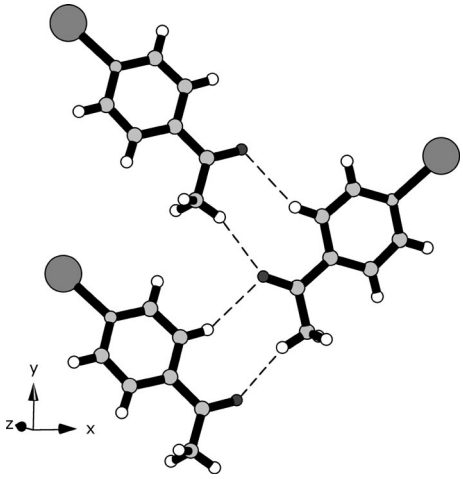

Figure 6. The weak hydrogen bonds connecting the 2D grids in **2** result in "tapes" (or a zipper) connecting the 2D nets.

Another difference is that the sheets are now both parallel and stacked exactly on top of each other. This means that the Fe^{II} ions are approximately ordered in a primitive-"cubic" arrangement where one side is much longer [11.5723(2) Å].

Magnetic Measurements

$[Fe^{II}(pyridine)_2(N_3)_2(H_2O)]$ (1)

Upon cooling the χT product decreases from a value of 3.80 $cm^3\,K\,mol^{-1}$ at 300 K to a minimum value of 2.50 $cm^3\,K\,mol^{-1}$ at ca. 20 K. From this temperature χT increases sharply to reach a maximum at ca. 6 K, and this value is dependent on the applied field (Figure 7). χT decreases when lowering the temperature, which may be ascribed to saturation effects of the magnetization. Above 30 K, the $1/\chi$ vs. T plot is well fitted to a Curie–Weiss law $C/(T - \theta)$ with $\theta = -20$ K. The Curie constant, C = 4.02 $cm^3\,K\,mol^{-1}$, agrees with the value expected for a high spin Fe^{II} ion with $g = 2.30$.

The decrease in χT in the range 300–20 K as well as the negative sign of θ should be ascribed to antiferromagnetic interactions operative between the Fe^{II} ions above 30 K. This is in agreement with the EE bridging mode of the azido groups in compound **1**, which is known to generally favour antiferromagnetic couplings.[7,19] This high tempera-

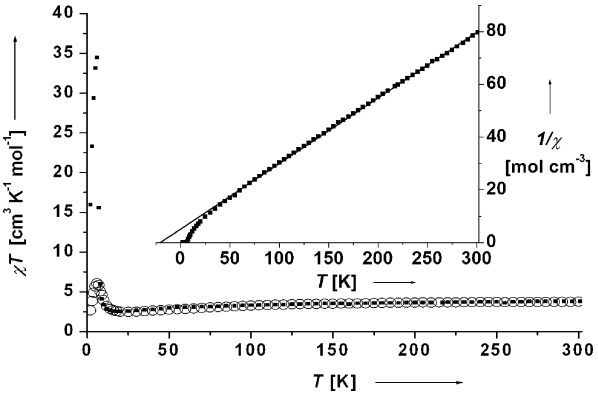

Figure 7. χT vs. T measured with an applied magnetic field of 5 kG (open circles) and 0.5 kG (black square) on a polycrystalline sample of $[Fe^{II}(pyridine)_2(N_3)_2(H_2O)]$ (**1**). The inset shows $1/\chi$ vs. T at 0.5 kG.

ture behaviour combined with the sharp increase of χT below 6 K is at a first glance reminiscent of spontaneous ordering in ferrimagnetic materials. However, a ferrimagnetic behaviour in compound **1** would require different Fe^{II} topologies as has been previously reported for some azido-bridged Mn^{II} compounds.[20–22] This is not the case. Indeed, compound **1** is a 1D compound with all the Fe^{II} ions bridged by the azido groups in the EE mode. Thus such behaviour for compound **1** is better ascribed to weak ferromagnetism resulting from spin canting as reported for another azido-bridged Mn^{II} compound.[23]

Weak ferromagnetism from spin canting is well evidenced from the field dependence of the magnetization at 2 K (Figure 8), which increases sharply between 0–1 kG to a value of about 1.0 μ_B whereby an inflexion point is observed. From this point the magnetization continuously increases, which may be ascribed to spin-flop transitions, but does not reach saturation at the highest measured magnetic field of 55 kG (ca. 2 μ_B) and no hysteresis loop is evidenced at 2 K. From the value of the magnetization before the spin flop (μ_w = 1.0 μ_B), which is only a fraction of the expected saturation value (μ_S = 4.6 μ_B for g = 2.3), we can estimate the spin-canting angle $\alpha = \sin^{-1}(\mu_w/\mu_S)$ to be ca. 13°.[24]

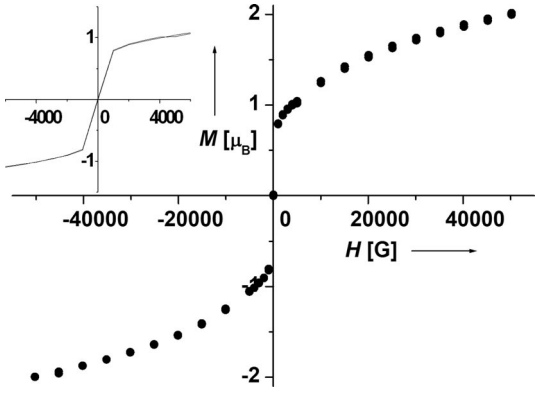

Figure 8. $M(H)$ vs. H measured at 2 K on a polycrystalline sample of $[Fe^{II}(pyridine)_2(N_3)_2(H_2O)]$ (**1**).

$[Fe^{II}(4\text{-acetylpyridine})_2(N_3)_2]$ (2)

At 300 K the χT product has a value of 3.60 $cm^3\,K\,mol^{-1}$ and decreases upon cooling to reach a minimum value of 2.80 $cm^3\,K\,mol^{-1}$ at 45 K. From this temperature χT increases sharply and reaches a maximum at ca. 17 K. The χT value of the maximum is dependent on the applied field (Figure 9). Below 17 K χT decreases, which may also be ascribed to saturation effects of the magnetization. The $1/\chi$ vs. T plot is fitted to a Curie–Weiss law above 50 K with θ = –27 K. The Curie constant C = 3.62 $cm^3\,K\,mol^{-1}$ agrees well with the value expected for the Fe^{II} ion with a slightly anisotropic g value (g = 2.20). The θ value is close to the one reported (θ = –26 K) for the 3D EE azido-bridged Fe^{II} polymorph of $[Fe(N_3)_2(4,4'\text{-bipyridine})]$.[16] This agrees well with the Fe···Fe separation of 5.902 Å found in this compound,[16] close to those in compound **2**.

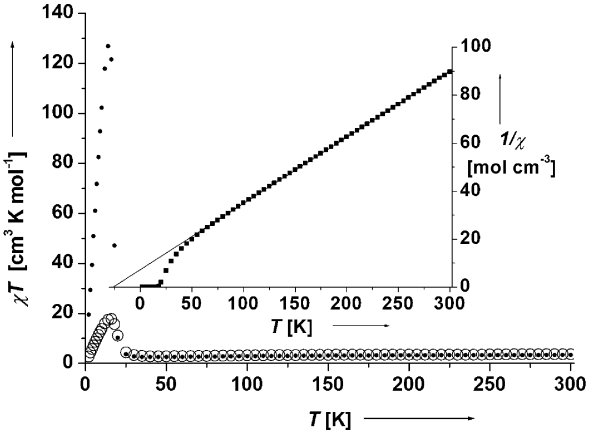

Figure 9. χT vs. T measured with an applied magnetic field of 5 kG (open circles) and 0.5 kG (black circles) on a polycrystalline sample of $[Fe^{II}(4\text{-acetylpyridine})_2(N_3)_2]$ (**2**). The inset shows $1/\chi$ vs. T at 0.5 kG.

As for compound **1**, the decrease of χT and the negative sign of θ at high temperature are due to the antiferromagnetic coupling of the Fe^{II} ions by the azido ligands in the EE bridging mode. Here again the sudden increase below 45 K should be ascribed to the signature of weak ferromagnetism resulting from spin canting.

This is also evidenced from the field dependence of the magnetization (Figure 10) at 2 K, which as for compound **1** increases sharply between 0–1 kG to a value of 1.2 μ_B whereby it shows an inflexion point and then increases continuously without reaching saturation at 55 kG (2 μ_B). However, in contrast with compound **1** a hysteresis loop is observed at this temperature (2 K) with a coercive field of 0.7 kG. From the value of the magnetization before the spin flop (1.2 μ_B) we estimate the spin canting angle α to be of the same order (ca. 15°) as for compound **1**.

In **1** and **2** the canting may be due to a lack of a centre of symmetry between the Fe^{II} ions thus allowing the required antisymmetric exchange.[25]

As a first interpretation, the appearance of spontaneous canted ferromagnetic ordering at a higher temperature for compound **2** (ca. 45 K) than for **1** (ca. 20 K), as well as the

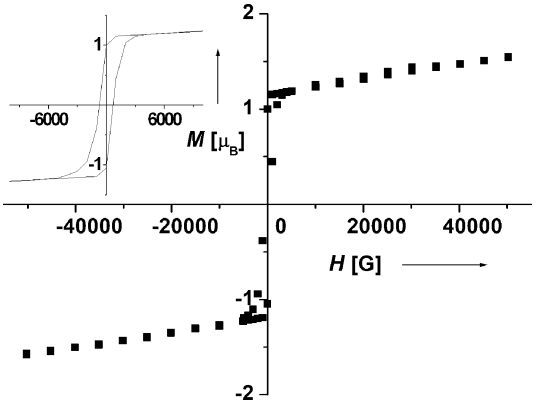

Figure 10. $M(H)$ vs. H measured at 2 K on a polycrystalline sample of $[Fe^{II}(4\text{-acetylpyridine})_2(N_3)_2]$ (**2**).

observation of a hysteresis loop for **2** at 2 K but not for **1**, could be ascribed to the increase in dimensionality of the azido-bridged Fe^{II} network. However, this is misleading as the previously reported 3D azido-bridged Fe^{II} polymorph of $[Fe(N_3)_2(4,4'\text{-bipyridine})]$[16] has magnetic data that are almost superimposable with those of our 2D compound **2**.

In the three compounds the azido bridges are in the EE mode. If one looks at the length of the pathway for Fe···Fe magnetic interactions they are almost identical for the three compounds (ca. 6.6 Å). However, in **1** the azido group bridges in a *cis* conformation whereas it is *trans* in compound **2** and in the 3D compounds reported by Fu et al.[16] This is the reason why the Fe ions are brought closer in **1** [5.4763(1) Å] than in **2** [5.9023(1) Å] and Fu's 3D compound (5.867 Å).[16] The weaker antiferromagnetic coupling in **1** (θ = –20 K) than in **2** (θ = –27 K) is difficult to interpret considering only one structural parameter. Indeed the studies of the EE azido bridge, particularly for the copper(II) systems, have shown that the magnetic coupling is very sensitive to small changes in several structural parameters such as the coordination geometry,[26] the Cu–N bond lengths or the Cu–N···N–Cu torsion angle as recently pointed out.[27] For Fu's 3D compounds and compound **2** the same strength of the antiferromagnetic coupling (θ = –27 K) is in agreement with their close structural parameters.

Spin density studies using polarized neutron diffraction may bring about better insight into the mechanism, as has been shown for Cu^{II}–azide dimers.[28,29]

Topological Analysis of $^3[Fe(N_3)_2(4,4'\text{-bipyridine})]$[16]

While comparing these two sets of structures and magnetic measurements we also found that the topology of the 3D polymorph of $[Fe(N_3)_2(4,4'\text{-bipyridine})]$ was quite remarkable. As pointed out by Fu et al.,[16] and by Han et al. for the isostructural Mn^{II} compound,[23] these compounds have a unique network structure, see Figure 11. Network topologies (3D nets) are important descriptors[30] in the rapidly moving field of 3D-coordination polymers and metal-organic frameworks,[31–34] and it is rare to find new simple nets in very symmetric coordination polymers.[35]

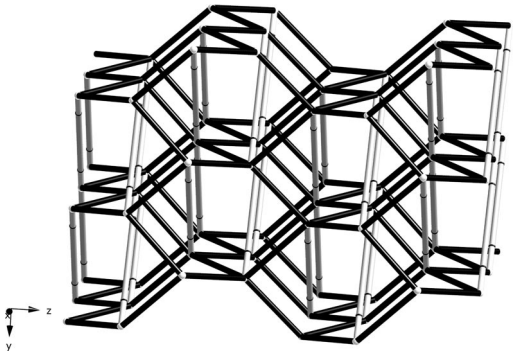

Figure 11. Analysis of the network structure in the 3D polymorph of $[Fe(N_3)_2(4,4'\text{-bipyridine})]$[16] gives a diamond net (**dia**) in black where the linkers are azide ions, supported by additional 4,4′-bipyridine linkers in light grey giving a six-connected net with $(5^{10}\cdot6^4\cdot7)$-**jsm** topology.

In this case it is important to note that the magnetic interactions in these compounds are likely transmitted by the azide ions, and thus the *magnetic network* is of the very common diamond (**dia**) topology.

If we add the 4,4′-bipyridine links to this we indeed get an unprecedented uninodal **six-connected** 3D net with the short (Schläfli) symbol: $5^{10}\cdot6^4\cdot7$ given the code (symbol) **jsm**.[36]

There is a synthetic implication of this that may be important. We may interpret this structure as a diamond net supported by bracing wires made up of 2,2′-bipyridines. This gives us a new possibility in the preparation of 3D-coordination polymers: (1) Design a network based on "unsaturated" metal-ion nodes and our principal bridging ligands. (2) Measure the distance and geometric constraints between the unsaturated nodes and find a suitable complimentary bridging ligand to insert into the network.

This strategy is somewhat similar to the use of templating molecules or ions. However, it will put more restrictions on the metal site, but may on the other hand prove to be more reliable when it comes to predicting the structures.

Conclusions

We have prepared two Fe^{II} azides with 1D and 2D topologies both displaying canted ferromagnetism in agreement with their structural features and other recent findings of Fe^{II} and Mn^{II} azides. In addition we have assigned the new network topology **jsm** to some related 3D M^{II} azides.

Experimental Section

Materials and Instrumentation: All chemicals and solvents were of analytical grade and used as received without further purification. All preparations and manipulations were performed under aerobic conditions. Electronic spectra of solid samples mulled in Nujol

were measured over the range 280–1050 nm with a Pye Unicam spectrophotometer, model SP 8000.

X-ray Crystallography: Crystallographic measurements were performed with a Siemens Smart CCD diffractometer with graphite-monochromated Mo-K_α radiation at 173 K. The structures were solved by direct methods and subsequent full-matrix least-squares refinement, including anisotropic thermal parameters for all non-hydrogen atoms. Hydrogen atoms were refined isotropically with the use of geometrical constraints. The calculations were carried out with the SHELXTL program package.[37] CCDC-650316 (for **1**) and -650317 (for **2**) contain the supplementary crystallographic data for this paper. These data can be obtained free of charge from The Cambridge Crystallographic Data Centre via www.ccdc.cam.ac.uk/data_request/cif.

Network Analysis: The short (Schläfli) symbol describes the number of smallest rings found in the net, and also gives the stoichiometry and the connectivity (p) of the nodes, {through the relation: $p = 1/2 + [1/4 + 2\cdot(\text{sum of superscripts})]^{0.5}$} and thus gives a rough idea of the type of network in question. The short (Schläfli) symbol, the vertex (or long) symbol and the C10 (td10) value were calculated using the program TOPOS,[38,39] giving for the 3D net in $[M^{II}(N_3)_2(4,4'\text{-bipyridine})]$[16,23] $5^{10}\cdot6^4\cdot7$ and $5\cdot5\cdot5_2\cdot5_2\cdot5_2\cdot5_2\cdot5_2\cdot5_2\cdot5_3\cdot5_3\cdot6\cdot6\cdot6\cdot*$ and 3912. This net is now found in the Reticular Chemistry Structure Resource[37] database under the code **jsm**.

Magnetic Measurements: Magnetic data were recorded using a Quantum Design SQUID magnetometer. To avoid orientation in the magnetic field the samples were pressed in a home-made Teflon sample holder equipped with a piston. The data were corrected for diamagnetism of the constituent atoms using Pascal's constants.

Caution! *Azide compounds are potentially explosive! Only a small amount of material should be prepared and handled with care.*

***Catena*-$[Fe^{II}(\mu_{1,3}\text{-}N_3)(N_3)(\text{pyridine})_2(H_2O)]$ (1):** A few drops of a saturated aqueous solution of L-ascorbic acid were added to a cold aqueous solution of $FeSO_4\cdot7H_2O$ (0.56 g, 2 mmol, 25 cm^3), followed by the addition of a solution of pyridine (0.32 g, ca. 4.0 mmol, 10 cm^3) in ethanol. Further, an aqueous solution of NaN_3 (0.65 g, 10 mmol, 10 cm^3) was added drop by drop with continuous stirring. The deep red solution was allowed to stand in a refrigerator for a couple of days. Deep-red crystals, suitable for X-ray measurements, of *catena*-$[Fe(\mu_{1,3}\text{-}N_3)(N_3)(py)_2(H_2O)]_n$ (**1**) were obtained with a yield of 0.60 g, ca. 70% with respect to iron. $C_{10}H_{12}FeN_8O$ (316.12): calcd. C 37.99, H 3.82, Fe 17.7, N 35.46; found C 38.42, H 3.82, Fe 18.3, N 34.88. IR spectrum (KBr pellet): $\tilde{\nu}$ = 3409 (s), 20735 (vs), 1643 (wm), 1596 (s), 1485 (ms), 1441 (s), 1384 (ms), 1219 (ms), 1156 (ms), 1073 (s), 1036 (s), 1008 (ms), 756 (ms), 701 (s), 664 (wm), 627 (m), 598 (m), 410 (wm), 387 (wm), 365 (wm), 342 (m), 319 (ms), 296 (ms), 269 (s), 232 (vs) cm^{-1} (v = very, s = strong, m = medium, w = weak, br = broad).

$[Fe^{II}(N_3)_2(\text{4-acetylpyridine})_2]_n$ (2): This complex was synthesized by mixing a solution of 4-acetylpyridine (1.0 mL, 4.46 mmol) in ethanol (6.0 mL) with a solution of $FeSO_4\cdot7H_2O$ (0.56 g, 2.0 mmol) in an ice cold aqueous solution (25 mL) containing a few drops of an aqueous saturated solution of L-ascorbic acid, followed by the dropwise addition of an aqueous solution (2 mL) of NaN_3 (0.65 g, 10.0 mmol) with constant stirring. The red mixture was allowed to stand in a refrigerator at ca. 4 °C for several days until good quality orange crystals of complex **2** were obtained with a yield of 0.76 g, ca. 75% with respect to iron. $C_{14}H_{14}FeN_8O_2$: calcd. C 44.00, H 3.69, N 29.32; found C 43.45, H 3.52, N 28.98. IR spectrum (KBr pellet): $\tilde{\nu}$ = 3368 (wm), 3075 (w), 2099 (vs), 2075 (vs), 1688 (vs), 1645 (wm), 1593 (wm), 1475 (wm), 1428 (ms), 1368 (s), 1333 (wm), 1281 (s), 1249 (s), 1200 (ms), 1043 (m), 1019 (wm), 803 (wm), 694 (s), 646 (wm), 585 (ms), 476 (w), 428 (w), 409 (w), 387 (w), 366 (w), 315 (w), 292 (m), 270 (s) cm^{-1}.

Electronic Spectra: The recorded spectrum for **1** shows a strong band at 354 nm attributed to the inter-ligand absorption and a shoulder at 415 nm represents a charge-transfer transition while the d–d transition appears very broad with lower intensity at λ_{max} = 906 nm. Complex **2** shows similar peaks at around 340, 480 and 1000 nm, in agreement with earlier data.[40] The broad, or split, spin-allowed $^5T_{2g} - {}^5E_{2g}$ transition bands above 800 nm are well known in O_h symmetry of iron(II) complexes.

Acknowledgments

We are grateful for financial support from the Swedish Science Council and the Swedish International Development Agency. Funding and instrumental support for magnetic measurements were provided by the "Commissariat à l'Energie Atomique" (CEA) through the "Laboratoire de Recherche Conventioné" (LRC No. DSM-03-31). L. Ö. is grateful for a travel grant to Lyon from the Knut and Alice Wallenberg Foundation. We thank Prof. Michael O'Keeffe for checking the **jsm** net and adding it to the RCSR database.

[1] S. J. Blundell, F. L. Pratt, *J. Phys.: Condens. Matter* **2004**, *16*, R771–R828.
[2] R. Winpenny, *Single-Molecule Magnets and Related Phenomena* in *Structure and Bonding*, vol. 122, Springer, Berlin, **2006**.
[3] R. Jain, K. Kabir, J. B. Gilroy, K. A. R. Mitchell, K. C. Wong, R. G. Hicks, *Nature* **2007**, *445*, 291–294.
[4] J. S. Miller, *Inorg. Chem.* **2000**, *39*, 4392–4408.
[5] T. Mallah, S. Thiébaut, M. Verdaguer, P. Veillet, *Science* **1993**, *262*, 1554–1557.
[6] V. Gadet, T. Mallah, I. Castro, M. Verdaguer, P. Veillet, *J. Am. Chem. Soc.* **1992**, *114*, 9213–9214.
[7] The most recent review seems to be: J. Ribas, A. Escuer, M. Monfort, R. Vicente, R. Cortes, L. Lezama, T. Rojo, *Coord. Chem. Rev.* **1999**, *195*, 1027–1068.
[8] C. M. Liu, S. Gao, D. Q. Zhang, Y. H. Huang, R. G. Xiong, Z. L. Liu, F. C. Jiang, D. B. Zhu, *Angew. Chem. Int. Ed.* **2004**, *43*, 990–994.
[9] F. C. Liu, Y. F. Zeng, J. Jiao, X. H. Bu, J. Ribas, S. R. Batten, *Inorg. Chem.* **2006**, *45*, 2776–2778.
[10] G. Leibeling, S. Demeshko, S. Dechert, F. Meyer, *Angew. Chem. Int. Ed.* **2005**, *44*, 7111–7114.
[11] A. Escuer, F. A. Mautner, M. A. S. Goher, M. A. M. Abu-Youssef, R. Vicente, *Chem. Commun.* **2005**, 605–607.
[12] Y. F. Zeng, F. C. Liu, J. P. Zhao, S. Cai, X. H. Bu, J. Ribas, *Chem. Commun.* **2006**, 2227–2229.
[13] P. Gutlich, H. A. Goodwin, *Spin crossover – An overall perspective*, vol. 233, Springer, Berlin, **2004**, pp. 1–47.
[14] R. Feyerherm, A. Loose, T. Ishida, T. Nogami, J. Kreitlow, D. Baabe, F. J. Litterst, S. Sullow, H. H. Klauss, K. Doll, *Phys. Rev. B* **2004**, 69.
[15] Y. Morishita, Y. Doi, T. Nogami, T. Ishida, *Chem. Lett.* **2006**, *35*, 770–771.
[16] A. H. Fu, X. Y. Huang, J. Li, T. Yuen, C. L. Lin, *Chem. Eur. J.* **2002**, *8*, 2239–2247.
[17] A. Escuer, R. Vicente, M. A. S. Goher, F. A. Mautner, *Inorg. Chem.* **1995**, *34*, 5707–5708.
[18] M. A. M. Abu-Youssef, F. A. Mautner, R. Vicente, *Inorg. Chem.* **2007**, *46*, 4654–4659.
[19] A. Escuer, G. Aromi, *Eur. J. Inorg. Chem.* **2006**, 4721–4736.
[20] M. A. M. Abu-Youssef, A. Escuer, M. A. S. Goher, F. A. Mautner, G. J. Reiss, R. Vicente, *Angew. Chem. Int. Ed.* **2000**, *39*, 1624.

[21] M. A. M. Abu-Youssef, M. Drillon, A. Escuer, M. A. S. Goher, F. A. Mautner, R. Vicente, *Inorg. Chem.* **2000**, *39*, 5022–5027.
[22] A. K. Ghosh, D. Ghoshal, E. Zangrando, J. Ribas, N. R. Chaudhuri, *Inorg. Chem.* **2005**, *44*, 1786–1793.
[23] S. Han, J. L. Manson, J. Kim, J. S. Miller, *Inorg. Chem.* **2000**, *39*, 4182–4185.
[24] O. Kahn, *Molecular magnetism*, VCH Verlagsgesellschaft, Weinheim, **1993**.
[25] T. Moriya, *Phys. Rev.* **1960**, *120*, 91–98.
[26] F. F. de Biani, E. Ruiz, J. Cano, J. J. Novoa, S. Alvarez, *Inorg. Chem.* **2000**, *39*, 3221–3229.
[27] A. Escuer, M. Font-Bardia, S. S. Massoud, F. A. Mautner, E. Penalba, X. Solans, R. Vicente, *New J. Chem.* **2004**, *28*, 681–686.
[28] C. Aronica, E. Jeanneau, H. El Moll, D. Luneau, B. Gillon, A. Goujon, A. Cousson, M. A. Carvajal, V. Robert, *Chem. Eur. J.* **2007**, *13*, 3666–3674.
[29] M. A. Aebersold, B. Gillon, O. Plantevin, L. Pardi, O. Kahn, P. Bergerat, I. von Seggern, F. Tuczek, L. Öhrström, A. Grand, E. Lelièvre-Berna, *J. Am. Chem. Soc.* **1998**, *120*, 5238–5245.
[30] O. M. Yaghi, M. O'Keeffe, N. W. Ockwig, H. K. Chae, M. Eddaoudi, J. Kim, *Nature* **2003**, *423*, 705–714.
[31] N. R. Champness, *Dalton Trans.* **2006**, 877–880.
[32] M. O'Keeffe, O. M. Yaghi, *J. Solid State Chem.* **2005**, *178*, V–VI.
[33] L. Öhrström, K. Larsson, *Molecule-Based Materials: The Structural Network Approach*, Elsevier, Amsterdam, **2005**, p. 324.
[34] M. J. Rosseinsky, *Microporous Mesoporous Mater.* **2004**, *73*, 15–30.
[35] N. W. Ockwig, O. Delgado-Friedrichs, M. O'Keeffe, O. M. Yaghi, *Acc. Chem. Res.* **2005**, *38*, 176–182.
[36] M. O'Keeffe, O. M. Yaghi, S. Ramsden, *Reticular Chemistry Structure Resource*, Australian National University Supercomputer Facility, Canberra, **2007**, http://rcsr.anu.edu.au/.
[37] *SHELXTL Structure Determination Programs*, Bruker AXS Inc., Madison, Wisconsin, **2001**.
[38] V. A. Blatov, Ac.Pavlov St. 1, 443011 Samara, Russia, **2007**, http://www.topos.ssu.samara.ru/
[39] V. A. Blatov, A. P. Shevchenko, V. N. Serezhkin, *J. Appl. Crystallogr.* **2000**, *33*, 1193.
[40] M. A. S. Goher, M. A. M. Abu-Youssef, *Acta Chim. Hung.* **1987**, *124*, 749–758.

Received: June 21, 2007
Published Online: November 12, 2007

